A Novel Radiotracer for Molecular Imaging and Therapy of Gastrin-Releasing Peptide Receptor Positive Prostate Cancer

Ivica J. Bratanovic[1], Chengcheng Zhang[1], Zhengxing Zhang[1], Hsiou-Ting Kuo[1], Nadine Colpo[1], Jutta Zeisler[1], Helen Merkens[1], Carlos Uribe[2,3], Kuo-Shyan Lin[1, 2], François Bénard[1, 2]

[1]BC Cancer, 675 W 10th Ave, Vancouver, BC V5Z 1L3, Canada.
[2]Department of Radiology, University of British Columbia, 2775 Laurel Street, Vancouver, BC, V5Z 1M9
[3]Functional Imaging, BC Cancer, Vancouver, BC, Canada

First Author is a graduate student trainee.

Corresponding Author:
Francois Benard, M.D.
BC Cancer Research Institute
675 West 10th Avenue
Vancouver, BC, V5Z 1L3, Canada
Telephone: 604-675-8206
Email: fbenard@bccrc.ca

First Author:
Ivica Jerolim Bratanovic
675 West 10th Ave
Vancouver, BC, V5Z 1L3, Canada
Telephone: 250-889-0948
Email: ibratanovic@bccrc.ca

Running Title: *Radiotracers for GRPR Imaging*
Word Count: 4,942

DISCLOSURE

ABSTRACT

The gastrin-releasing peptide receptor (GRPR) is overexpressed in many solid malignancies, particularly in prostate and breast cancers, among others. We synthesized ProBOMB2, a novel bombesin derivative radiolabeled with ^{68}Ga and ^{177}Lu, and evaluated its ability to target GRPR in a preclinical model of human prostate cancer. **Methods:** ProBOMB2 was synthesized on solid phase using Fmoc chemistry. The chelator 1,4,7,10-tetraazacyclododecane-1,4,7,10-tetraacetic acid was coupled to the *N*-terminus and separated from the GRPR-targeting sequence by a cationic 4-amino-(1-carboxymethyl)-piperidine spacer. Binding affinity for both human and murine GRPR was determined using a cell-based competition assay, while a calcium efflux assay was used to measure the agonist/antagonist properties of the derivatives. ProBOMB2 was radiolabeled with ^{177}Lu and ^{68}Ga. SPECT and PET imaging, and biodistribution studies were conducted using a preclinical prostate cancer model of male immunocompromised mice bearing GRPR-positive PC-3 human prostate cancer xenografts. **Results:** Ga-ProBOMB2 and Lu-ProBOMB2 bound to PC-3 cells with a K_i of 4.58±0.67 and 7.29±1.73 nM, respectively. ^{68}Ga-ProBOMB2 and ^{177}Lu-ProBOMB2 were radiolabeled with a radiochemical purity greater than 95%. Both radiotracers were primarily excreted via the renal pathway. PET images of PC-3 tumor xenografts were visualized with excellent contrast at 1 h and 2 h post-injection (p.i.) with ^{68}Ga-ProBOMB2, and very low off-target organ accumulation. ^{177}Lu-ProBOMB2 enabled clear visualization of PC-3 tumor xenografts by SPECT imaging at 1 h, 4 h, and 24 h p.i. ^{177}Lu-ProBOMB2 displayed higher tumor uptake than ^{68}Ga-ProBOMB2 at 1 h p.i. ^{177}Lu-ProBOMB2 tumor uptake at 1 h, 4 h, and 24 h p.i. was 14.9±3.1, 4.8±2.1, and 1.7±0.3 %ID/g, respectively. **Conclusions:** ^{68}Ga-ProBOMB2 and ^{177}Lu-ProBOMB2 are promising radiotracers with limited pancreas uptake, good tumor uptake, and favorable pharmacokinetics for imaging and therapy of GRPR-expressing tumors.

Key Words: gastrin releasing peptide receptor, bombesin, prostate cancer

INTRODUCTION

The gastrin-releasing peptide receptor (GRPR) is a transmembrane G protein-coupled receptor that is expressed in the human body's central nervous system, gastrointestinal tract, pancreas, and adrenal cortex tissues(*1*). GRPR is also aberrantly overexpressed in many solid malignancies which include prostate, breast, lung, colon, and ovarian cancers(*2*). The overexpression of GRPR in cancer makes it an attractive target for radioligand imaging and therapy. In the past, GRPR antagonists based on bombesin (i.e., NeoBOMB1, RM2, and ProBOMB1) have been preferred over agonists due to adverse effects observed from using the latter(*3,4*).

NeoBOMB1 has recently been introduced in clinical trials to image and treat GRPR positive tumors with ^{68}Ga and ^{177}Lu labeled compounds, respectively(*5*). A common trend with GRPR targeting agents in patients and pre-clinical animal models is the high physiological accumulation of the radiotracer in the pancreas and gastrointestinal tract(*5,6*). The off-target accumulation of the radiotracer in normal organs can affect image contrast and lesion detection, and limit the maximum tolerated dose of radiotracer administered for radioligand therapy(*1*). Recently, our group began to address the issue of off-target GRPR binding (i.e., in the pancreas and intestines) with the development of ProBOMB1. It contains a unique terminal Leuψpro-NH$_2$ sequence that significantly reduced pancreas uptake compared to NeoBOMB1 while still retaining target specificity(*7,8*). However, ProBOMB1 displayed lower tumor uptake with ^{177}Lu label compared to NeoBOMB1, while ^{68}Ga-labeled tracer uptake was similar(*7,8*). To improve tumor uptake and further mitigate pancreas uptake, we designed, synthesized, and evaluated ProBOMB2 (Figure 1). ProBOMB2 contains the same GRPR binding sequence and unique terminal Leuψpro-NH$_2$ seen in ProBOMB1 but utilizes a cationic 4-amino-(1-carboxymethyl)-piperidine (Pip) spacer instead of a neutral *p*-aminomethylaniline-diglycolic acid spacer (Figure 1). The cationic Pip spacer has been used in the past with the GRPR antagonist ^{68}Ga-RM2 to improve tumor affinity and in our own lab to improve the pharmacokinetic profile of other radiotracers(*9,10*).

<!Figure-1-here!>

Herein, we describe the synthesis and pharmacokinetic evaluation of a novel bombesin derivative, ProBOMB2. We evaluated the potential of ProBOMB2 as a theranostic agent by radiolabeling with ^{68}Ga and ^{177}Lu. Antagonistic properties were evaluated using an *in vitro* fluorescence based Ca^{2+}

release assay. The pharmacokinetic properties of ^{68}Ga-ProBOMB2 and ^{177}Lu-ProBOMB2 were studied in a preclinical model of human prostate cancer.

MATERIALS AND METHODS

Synthesis of ProBOMB2 and Radiolabeling

ProBOMB2 was synthesized on solid-phase using a standard Fmoc-based approach. The synthesis of ProBOMB2 and its Lu and Ga cold standards is described in the Supplemental Information. ProBOMB2, Ga-ProBOMB2, and Lu-ProBOMB2 were purified by high-performance liquid chromatography and purity was confirmed by electrospray ionization-mass spectrometry (See Supplemental Information). ProBOMB2 was radiolabeled using [68]GaCl$_3$ to generate ^{68}Ga-ProBOMB2 and was purified using radio-high-performance liquid chromatography using the methods described in the Supplemental Information. [177]LuCl$_3$ was used to obtain ^{177}Lu-ProBOMB2, which was then purified using radio-high-performance liquid chromatography as described in the Supplemental Information. The molar activity of radiotracers was measured using high-performance liquid chromatography, by dividing the injected radioactivity by the tracer quantity, which was quantified by area under the UV absorbance peak and extrapolated from a standard curve. The standard curve was established with known quantities of non-radioactive Ga-ProBOMB2 or Lu-ProBOMB2.

Cell Culture

Human PC-3 prostate adenocarcinoma and murine Swiss 3T3 fibroblast cell lines were cultured and maintained in a humidified incubator (5% CO_2; 37°C) in F-12K medium and RPMI medium (Life Technologies Corporations), respectively, and supplemented with 10% fetal bovine serum, 100 I.U./mL penicillin, and 100 µg/mL streptomycin (Life Technologies). PC-3 cells were chosen due to their inherent propensity to display a high surface membrane density of human GRPR(11). Similarly, Swiss 3T3 cells were selected for their high surface density of murine GRPR as a way to further explain radiotracer biodistribution in our murine animal model(12).

Competition Binding Assay

The *In vitro* competition binding assays were conducted following previously published procedures, also described in the Supplemental Data(8).

Fluorometric Calcium Release Assay

The FLIPR Calcium 6 assay kit (Molecular Devices) was used to perform calcium release assays according to published procedures and are described in the Supplementary Data(*13*).

Animal Model

Animal experiments were approved by the Animal Care Committee of the University of British Columbia. For ^{68}Ga-ProBOMB2, 8-week old male NOD.Cg-Prkdc^{scid}Il2rg^{tm1Wjl}/SzJ mice were obtained from an in-house colony and were inoculated subcutaneously with $5x10^6$ PC-3 cells (100 µL; 1:1 PBS/Matrigel), and tumors were allowed to grow for 3 weeks. For ^{177}Lu-ProBOMB2, 8-week old male NOD.Cg-Rag1^{tm1Mom} Il2rg^{tm1Wjl}/SzJ were used instead, inoculated the same way as the NOD.Cg-Prkdc^{scid}Il2rg^{tm1Wjl}/SzJ mice.

PET/CT Imaging and Biodistribution Studies

Mice bearing PC-3 tumors were sedated (2.5% isoflurane in O_2) for intravenous injection of ^{68}Ga-ProBOMB2 (4.18±0.68 MBq) and allowed to recover and roam freely in their enclosure during the uptake period. Shortly before the imaging time, the mice were sedated again under isoflurane inhalation, and placed on the scanner (Inveon micro_PET/CT, Siemens Healthineers, USA) while body temperature was maintained using a heating pad. A baseline CT scan was obtained for localization and attenuation (80 kV; 500 µA; 300 ms) followed by a 10 min static PET scan at 1 or 2 h post-injection of the radiotracer. Following imaging, the mice were sacrificed under isoflurane anesthesia by CO_2 inhalation, for biodistribution analysis as described below.

The PET data were obtained in list mode, reconstructed using 3-dimensional ordered-subsets expectation maximization (2 iterations) and maximum a priori algorithm (18 iterations) with CT-based attenuation correction. The Inveon Research Workplace (IRW) software (Siemens Healthineers) was used to analyze and view the images. For biodistribution and blocking studies, the mice were injected with 1.47±1.17 MBq of radiotracer. At 1 h or 2 h, the mice were anesthetized with 2% isoflurane and euthanized by CO_2 inhalation. Blocking was done at 1 h via co-injection of the radiotracer with 100 µg of [D-Phe^6,Leu-NHEt^{13},des-Met^{14}]Bombesin(6-14). Blood was drawn via cardiac puncture, and the organs/tissues of interested were harvested, rinsed with saline, blotted dry, weighed, and counted using an automatic gamma counter (PerkinElmer). Uptake values were expressed as the percentage of the injected dose per gram of tissue (%ID/g).

SPECT/CT Imaging and Biodistribution Studies

PC-3 tumor bearing mice were sedated (2.5% isoflurane in O_2) and ^{177}Lu-ProBOMB2 (34.96±2.49 MBq) was administered intravenous. Prior to each SPECT/CT image acquisition, the mouse was given a subcutaneous injection of 250 μL of sterile saline for hydration. The same mouse was used for all imaging time-points. Mice were scanned while sedated (U-SPECT$^+$/CT, MI Labs, The Netherlands) using an extra ultra-high sensitivity big mouse collimator (2 mm pinhole size), while body temperature was maintained using a heating pad. The CT scan was obtained using 615 μA and 60 kV parameters for localization and attenuation, followed by a SPECT scan with a 20% energy window centered around 208 keV. Similarity regulated ordered subset expectation maximization (32 subsets, 4 iterations), 1.0 mm post-processing Gaussian filter, and a voxel size of 0.4 mm was used to reconstruct the images. Scatter correction was performed using the automatic triple energy window and a collimator dependent calibration factor was applied. Images were decay corrected to time of injection and divided by the injected activity with PMOD v 3.402 (PMOD Technologies, Switzerland), to obtain quantitation in %ID/g. Data was then converted to DICOM for visualization in IRW.

For biodistribution and blocking studies, the mice were injected with 2.50±0.62 MBq of radiotracer. At 1 h, 4, h, 24 h, or 72 h, the mice were anesthetized with 2% isoflurane and euthanized by CO_2 inhalation. Blocking was done at 1 h via co-injection of the radiotracer with 100 μg of [D-Phe[6],Leu-NHEt[13],des-Met[14]]Bombesin(6-14). Blood was drawn via cardiac puncture, and the organs/tissues of interested with collected, weighed, and counted using an automatic gamma counter (PerkinElmer). Uptake values were expressed as the percentage of the injected dose per gram of tissue (%ID/g).

Dosimetry

The uptake values (%ID/g) obtained from the biodistribution data were decayed to the appropriate time point and fitted to monoexponential or biexponential models using an in-house Python script (Python Software Foundation v.3.5). Biexponential fitting assumed zero uptake at t = 0. The best fit was picked based on the coefficient of determination (R^2) and by qualitatively looking at fits in log-log plots and its residuals. Time-activity curves were integrated to acquire residence times per unit gram and multiplied by mass of model tissue (25 g MOBY mouse phantom). The residence time data were input in OLINDA (Hermes Medical Solutions, v2.2) which has precalculated dose factors to obtain dosimetry(*14*,*15*).

Dosimetry estimations for average adult human male were extrapolated per published procedures(*8*).

Mouse biodistribution data was extrapolated to humans using the method proposed by Kirschner et al using the following equation(*16*):

$$\left(\frac{\%ID}{m_{organ}}\right)_{human} = \left(\frac{\%ID}{m_{organ}}\right)_{mouse}\left[\frac{M_{mouse}}{M_{human}} \times (m_{organ})_{human}\right]$$

Where m_{organ} is mass of organ and M represents total body mass. Once human equivalent biodistribution values were extrapolated with above equation, dosimetry was obtained as for the mouse case using OLINDA.

Statistical Analysis

Data analysis was conducted with GraphPad Prism 8.0. *t* tests were performed for all organs in the biodistribution studies and the binding affinity studies. For *t*-tests performed for organ comparison, a correction factor was used to account for multiple comparison using the Holm-Sidak method. Welch's *t* test was used to compare ProBOMB2 radiotracer accumulation in organs to each other and to previously established ProBOMB1 and NeoBOMB1 values. Statistically significant difference was considered present when the adjusted *p* value was < 0.05 using the Holm-Sidak method.

RESULTS

Chemistry and Radiolabelling

The starting material Fmoc-LeuψPro-OH was synthesized in solution phase with 31% yield. The precursor ProBOMB2 was synthesized using Fmoc chemistry on solid phase. The non-radioactive Ga-ProBOMB2 and Lu-ProBOMB2 were obtained in 88% and 86% yields, respectively. Multiple batches of ^{68}Ga-ProBOMB2 were prepared in good radiochemical yield (45.5±29.9%, n = 3) and good specific activity (139.86±70.67 GBq/μmol, n = 3), with > 95% radiochemical purity. ^{177}Lu-ProBOMB2 was prepared in good radiochemical yield (45.5±4.4%) and high specific activity (421.8±5.2 GBq/μmol), with > 99% radiochemical purity.

Binding Affinity and Antagonist Characterization

Ga-ProBOMB2 and Lu-ProBOMB2 binding affinities were measured in human GRPR expressing PC-3 prostate cancer cells and murine GRPR expressing Swiss 3T3 cells (Supplemental Figure 1 and Figure 2). The competitor ^{125}I-Tyr^{4}bombesin was successfully displaced in a dose dependent manner by

both compounds on PC-3 and Swiss 3T3 cells. K_i values for Ga-ProBOMB2 and Lu-ProBOMB2 on human GRPR expressing PC-3 cells were 4.58±0.67 and 7.29±1.73 nM, respectively (n = 3). K_i values for Ga-ProBOMB2 and Lu-ProBOMB2 on murine GRPR expressing Swiss 3T3 cells were 5.30±1.55 and 7.91±2.60 nM, respectively (n = 3). There was no significant difference in binding affinity for Ga-ProBOMB2 between murine and human GRPR (p = 0.528). Lu-ProBOMB2 also displayed no significant difference in the binding affinity between murine and human GRPR (p = 0.751).

Intracellular calcium release was measured for Ga-ProBOMB2 and Lu-ProBOMB2 using PC-3 cells (Supplemental Figure 3 and Supplemental Figure 4). Adenosine triphosphate (ATP) (50 nM) and bombesin (50 nM) induced Ca^{2+} efflux corresponding to 907.3±177.5 and 880.6±146.3 relative fluorescence units (RFUs), compared with 6.0±2.7 RFUs for buffer control. For [D-Phe[6],Leu-NHEt[13],des-Met[14]]Bombesin(6-14) (50 nM), 5.7±0.7 RFUs was observed. For Lu-ProBOMB2 (50 nM) 5.5±0.8 RFUs were recorded, while Ga-ProBOMB2 (50 nM) elicited 6.4±1.0 RFUs. Ga-ProBOMB2 RFUs were significantly lower from those of ATP (p = 0.002) and bombesin (p = 0.001) but were not significantly different from [D-Phe[6],Leu-NHEt[13],des-Met[14]]bombesin(6-14) (p = 0.299). Lu-ProBOMB2 RFUs were significantly lower than RFUs obtained with ATP (p = 0.002) and bombesin (p = 0.001) but were not significantly different from [D-Phe[6],Leu-NHEt[13],des-Met[14]]bombesin(6-14) (p = 0.719).

PET Imaging and Biodistribution

The PET and PET/CT images are shown in Figure 2. There was clear visualization of PC-3 tumor xenografts in mice by ^{68}Ga-ProBOMB2, which was excreted primarily through the renal pathway. The urine contained the highest activity of ^{68}Ga-ProBOMB2, followed by the tumor and kidneys, respectively. Co-injection of the blocking agent, [D-Phe[6],Leu-NHEt[13],des-Met[14]]Bombesin(6-14), reduced tumor uptake of ^{68}Ga-ProBOMB2 by 65% at 1 h p.i. This was a significant reduction in tumor uptake compared to the unblocked sample at 1 h p.i. (p = 0.0006).

<!Figure-2-here!>

PC-3 tumor uptake for ^{68}Ga-ProBOMB2 was 10.80±2.56 and 8.79±3.01 %ID/g at 1 h and 2 h p.i., respectively. There was no significant difference between 1 h and 2 h p.i. (p = 0.219). Kidney uptake for ^{68}Ga-ProBOMB2 was 1.81±0.44 and 1.27±0.31 %ID/g at 1 h and 2 h p.i., respectively. Blood, muscle, bone, and liver uptake of the PET tracer was <1 %ID/g across all time points (Figure 3). Pancreas uptake

was 1.20±0.42 and 0.30±0.11 %ID/g at 1 h and 2 h p.i., respectively. Tumor-to-blood ratio increased over time from 22.19±3.51 at 1 h to 75.32±28.59 at 2 h p.i. Tumor-to-kidney ratios were 6.03±0.88 and 6.96±1.89 at 1 h and 2 h p.i., respectively. Tumor-to-pancreas ratios increased from 9.32±1.38 to 31.05±9.28 from 1 h to 2 h p.i., respectively. Tumor-to-liver ratios remained high, increasing from 26.18±6.43 at 1 h to 34.99±16.10 at 2 h p.i. Complete biodistribution data is presented in Supplemental Table 1.

<!Figure-3-here!>

SPECT Imaging and Biodistribution

The maximum intensity projection SPECT images of ^{177}Lu-ProBOMB2 are shown in Figure 4. There was clear and high-contrast visualization of PC-3 tumor xenografts in mice by ^{177}Lu-ProBOMB2 at 1 h, 4 h, and 24 h, which was then excreted renally. The highest activity for ^{177}Lu-ProBOMB2 was observed in the urine, followed by the tumor and kidneys. Co-injection of the blocking agent, [D-Phe[6],Leu-NHEt[13],des-Met[14]]Bombesin(6-14), decreased tumor uptake of ^{177}Lu-ProBOMB2 by 80% at 1 h p.i.

<!Figure 4 near here!>

PC-3 tumor uptake for ^{177}Lu-ProBOMB2 was 14.94±3.06, 4.75±2.06, 1.68±0.30, and 0.91±0.15 %ID/g at 1, 4, 24, and 72 h p.i., respectively. Kidney uptake for ^{177}Lu-ProBOMB2 was 2.44±0.59 %ID/g at 1 h p.i., which by 24 h p.i. dropped to 0.71±0.10 %ID/g. Pancreas uptake was 1.36±0.45 %ID/g at 1 h p.i., and at 4 h p.i. descended to 0.17±0.06 %ID/g. Blood, muscle, bone, and liver uptake of the SPECT tracer was < 1 %ID/g across all time points (Figure 5). Biodistribution data for all other collected organs is presented in Supplemental Table 2. Tumor-to-blood ratio increased over time from 35.34±8.47 at 1 h to 320.13±160.30 at 24 h p.i. Tumor-to-kidney ratios peaked at 6.33±1.60 at 1 h p.i., decreasing to 2.39±0.30 at 24 h p.i. Tumor-to-pancreas ratios increased from 11.70±3.08 at 1 h p.i. to 19.57±4.00 at 24 h p.i. Tumor-to-liver ratios peaked with 54.73±12.31 at 1 h p.i., decreasing to 13.77±4.50 at 24 h p.i.

<!Figure-5-here!>

Dosimetry

The absorbed doses in mice injected with ^{177}Lu-ProBOMB2 are shown in Table 1. The bladder received the highest dose, followed by the PC-3 tumor and the kidneys.

<!Table-1-here!>

Table 2 lists the estimated absorbed whole-body dose for an average adult male. This data remained consistent with the mouse model. The highest estimated normal organ dose was observed in the urinary bladder with, followed by the kidneys. The estimated pancreas dose remained low, along with other tissues of interest (e.g. gastrointestinal tract).

<!Table-2-here!>

DISCUSSION

GRPR is an attractive radiopharmaceutical target for cancer therapy and diagnosis due to its overexpression in many cancer types(*1*,*17–19*). Bombesin based GRPR antagonists can image both primary and metastatic disease in patients, particularly in estrogen receptor positive breast cancer and prostate cancer(*5*,*6*,*8*,*20–22*). The literature largely supports the use of GRPR radiotracers for prostate cancer, where it can be combined with prostate-specific membrane antigen radiopharmaceuticals to enhance disease management(*19*,*23*). Some bombesin based radiotracers often accumulate in the intestine and pancreas, negatively affecting tumor contrast(*24*,*25*). Incorporating a charged hydrophilic linker in the radiotracer sequence can increase water solubility, renal excretion, and tumor uptake of radiopharmaceuticals to enhance image contrast(*26*,*27*). Novel ^{177}Lu-ProBOMB2 and ^{68}Ga-ProBOMB2 contained the unique terminal LeuψPro moiety used in ProBOMB1 but now include a cationic Pip spacer to improve tumor uptake and contrast(*7*,*8*).

Ga-ProBOMB2 and Lu-ProBOMB2 were found to be potent GRPR antagonists, highly desirable for tolerability in humans as it will reduce undesirable effects(*3*,*4*). ^{68}Ga-ProBOMB2 and ^{177}Lu-ProBOMB2 demonstrated high-contrast visualization of GRPR-expressing PC-3 prostate cancer xenografts with minimal normal organ uptake on PET and SPECT imaging, respectively. Both radiotracers were rapidly excreted from the blood and peripheral organs through the renal pathway. Blocking studies confirmed radiotracer specificity for GRPR. While blocking was not complete, decreasing tumour uptake from 10.8 %ID/g to 3.77 %ID/g, this likely reflected an insufficient dose of the blocking competitor, [D-Phe6,Leu-NHEt13,des-Met14]-Bombesin, and/or differences in the clearance profile of the competitor relative to the radioligand.   Complete biodistribution studies corroborated the quality of the PET and SPECT images, indicating high rapid normal organ clearance of the radiotracers (Figures 2 and 4). Peak tumor uptake was at 1 h p.i. for both the ^{68}Ga and ^{177}Lu radiotracers, each with minimal pancreas and kidney uptake.

These are unique outcomes, as previous GRPR antagonists characteristically have significant pancreas and normal organ accumulation (i.e. RM2 and NeoBOMB1)([19,20]). Our ProBOMB2 radiotracers have an inherent specificity for GRPR positive cancer tissue but not healthy tissue that expresses GRPR (i.e. the pancreas). Our binding affinity experiments show that that the lack of pancreas and intestine uptake is not due to the interspecies difference in GRPR structure of our animal model, rather it is a unique property of ProBOMB2 which warrants further investigation.

The biodistribution of ^{68}Ga-ProBOMB2 compared to ^{68}Ga-NeoBOMB1 found that at 1 h p.i. there was a significantly lower retention of ^{68}Ga-ProBOMB2 in non-target tissues, such as the blood, intestines, stomach, liver, pancreas and kidneys ($p < 0.05$), while maintaining similar tumor uptake ($p > 0.05$) (Figure 6)([8]). The same pattern was observed when comparing ^{177}Lu-ProBOMB2 to ^{177}Lu-NeoBOMB1. The significantly higher tumor uptake for ^{177}Lu-ProBOMB2 compared to ^{177}Lu-NeoBOMB1 ($p < 0.05$) at 1 h p.i. is a promising characteristic, as there was significantly lower uptake of our radiotracer in the blood, intestine, pancreas, and liver ($p < 0.05$) (Figure 6)([7]). However, ^{177}Lu-ProBOMB2 had significant washout from the tumor at 4 h p.i., resulting in lower tumor uptake compared to ^{177}Lu-NeoBOMB1 (Figure 6). The GRPR radiotracer profile of high pancreas uptake is also observed in RM2, a clinically established GRPR specific radiotracer([22]). ^{68}Ga-RM2 presented with notably high pancreas uptake in both pre-clinical and clinical studies([20,22]). Using the same prostate cancer model as our study, ^{68}Ga-RM2 achieved similar tumor uptake at 1 and 2 h p.i., but had higher pancreatic accumulation([20]).

<!Figure-6-here!>

Both ^{177}Lu-ProBOMB2 and ^{68}Ga-ProBOMB2 are strong candidates for clinical translation. They demonstrated rapid clearance, resulting in high tumor-to-blood, -bone, and -muscle ratios. Importantly, a high tumor-to-pancreas was obtained, the common dose limiting organ for ^{177}Lu-RM2 and ^{177}Lu-NeoBOMB1([5,28]). ProBOMB2 is a GRPR antagonist, and there was washout of the radiotracer from the tumor over time. Sustained tumor uptake is desirable to enhance relative radiation dose delivered to tumors relative to normal organs. Further improvements in tumor retention may be achieved by improving the metabolic stability of bombesin derivatives.

ProBOMB2 was primarily excreted renally, leading to the bladder receiving the highest absorbed dose in our mouse model, followed by the kidneys (Table 2). This is likely due to high blood and tumor

clearance of our radiotracer. In future iterations, this can be improved upon by increasing the radiotracer's biological half-life using albumin binders to attenuate bladder dosing and mitigate tissue damage. The remaining organs remained low and comparable to each other. When compared to published data for ^{177}Lu labeled NeoBOMB1 and ProBOMB1, the predicted dose for a human adult male was much lower for many key organs with ^{177}Lu-ProBOMB2 (Figure 7). The average male would be expected to receive approximately 100 times less dose to the pancreas with ^{177}Lu-ProBOMB2 compared to ^{177}Lu-NeoBOMB1.

<!Figure-7-here!>

The favorable distribution profile of ProBOMB2 has the potential to reduce radiation exposure to normal organs and is a promising alternative for therapy of GRPR positive cancers.

CONCLUSION

We synthesized ProBOMB2, a novel GRPR targeting peptide with nanomolar affinity for the receptor, and successfully radiolabeled it with ^{68}Ga and [177]Lu. [68]Ga- and ^{177}Lu-ProBOMB2 were able to provide high-contrast images of GRPR-expressing tumors in a preclinical human prostate cancer model with PET and SPECT, respectively, with minimal pancreas uptake. With high tumor to pancreas and normal organ uptake ratios and favorable dosimetry, [68]Ga- and ^{177}Lu-ProBOMB2 warrant further investigation as a theranostic pair for cancer imaging and therapy.

KEY POINTS:

QUESTION: How well does the novel peptide ProBOMB2 bind to GRPR and allow imaging of GRPR positive cancers when radiolabelled with either ^{68}Ga or ^{177}Lu?

PERTINENT FINDINGS: ProBOMB2 was radiolabelled with ^{68}Ga or ^{177}Lu and accumulated specifically in GRPR positive neoplastic tissue, with minimal normal organ uptake. There was significantly less uptake in the pancreas compared to previous GRPR targeting radiopeptides (i.e. NeoBomb1) while maintaining sustained tumor uptake.

IMPLICATIONS FOR PATIENT CARE: ProBOMB2 can accumulate in GRPR positive neoplasms with lower uptake in healthy tissues (i.e. the pancreas) to improve image contrast for diagnostic use and reduce off-target tissue damage for therapeutic applications.

REFERENCES

1. Jensen RT, Battey JF, Spindel ER, Benya R V. International Union of Pharmacology. LXVIII. Mammalian Bombesin Receptors: Nomenclature, Distribution, Pharmacology, Signaling, and Functions in Normal and Disease States. *Pharmacol Rev*. 2008;60:1-42.

2. Cornelio DB, Roesler R, Schwartsmann G. Gastrin-releasing peptide receptor as a molecular target in experimental anticancer therapy. *Ann Oncol*. 2007;18:1457-1466.

3. Cescato R, Maina T, Nock B, et al. Bombesin receptor antagonists may be preferable to agonists for tumor targeting. *J Nucl Med*. 2008;49:318-326.

4. Bodei L, Ferrari M, Nunn A, et al. 177Lu-AMBA bombesin analogue in hormone refractory prostate cancer patients: a phase I escalation study with single-cycle administrations. *Eur J Nucl Med Mol Imaging*. 2007;34:S221-S221.

5. Dalm SU, Bakker IL, De Blois E, et al. 68Ga/177Lu-NeoBOMB1, a novel radiolabeled GRPR antagonist for theranostic use in oncology. *J Nucl Med*. 2017;58:293-299.

6. Zang J, Mao F, Wang H, et al. 68Ga-NOTA-RM26 PET/CT in the Evaluation of Breast Cancer : A Pilot Prospective Study. *Clin Nucl Med*. 2018;43:663-669.

7. Rousseau E, Lau J, Zhang Z, et al. Comparison of biological properties of [177 Lu]Lu-ProBOMB1 and [177 Lu]Lu-NeoBOMB1 for GRPR-targeting. *J Label Compd Radiopharm*. 2019;1:0-2.

8. Lau J, Rousseau E, Zhang Z, et al. Positron Emission Tomography Imaging of the Gastrin-Releasing Peptide Receptor with a Novel Bombesin Analogue. *ACS Omega*. 2019;4:1470-1478.

9. Zhang Z, Amouroux G, Pan J, et al. Radiolabeled B9958 Derivatives for Imaging Bradykinin B1 Receptor Expression with Positron Emission Tomography: Effect of the Radiolabel-Chelator Complex on Biodistribution and Tumor Uptake. *Mol Pharm*. 2016;13:2823-2832.

10. Zhang C, Zhang Z, Lin KS, et al. Preclinical melanoma imaging with 68Ga-labeled α-melanocyte-stimulating hormone Derivatives using PET. *Theranostics*. 2017;7:805-813.

11. Reile H, Armatis PE, Schally A V. Characterization of high-affinity receptors for bombesin/gastrin releasing peptide on the human prostate cancer cell lines PC-3 and DU-145: Internalization of receptor bound 125I-(Tyr4) bombesin by tumor cells. *Prostate*. 1994;25:29-38.

12. Zachary I, Rozengurt E. High-affinity receptors for peptides of the bombesin family in Swiss 3T3

cells. *Proc Natl Acad Sci U S A*. 1985;82:7616-7620.

13. Amouroux G, Pan J, Jenni S, et al. Imaging Bradykinin B1 Receptor with 68Ga-Labeled [des-Arg10]Kallidin Derivatives: Effect of the Linker on Biodistribution and Tumor Uptake. *Mol Pharm*. 2015;12:2879-2888.

14. Stabin MG, Sparks RB, Crowe E. OLINDA/EXM: The second-generation personal computer software for internal dose assessment in nuclear medicine. *J Nucl Med*. 2005;46:1023-1027.

15. Keenan MA, Stabin MG, Segars WP, Fernald MJ. RADAR realistic animal model series for dose assessment. *J Nucl Med*. 2010;51:471-476.

16. Kirschner AS, Ice RD, Beierwaltes WH. Radiation dosimetry of 131I 19 iodocholesterol. *J Nucl Med*. 1973;14:713-717.

17. Patel O, Shulkes A, Baldwin GS. Gastrin-releasing peptide and cancer. *Biochim Biophys Acta - Rev Cancer*. 2006;1766:23-41.

18. Nock BA, Kaloudi A, Lymperis E, et al. Theranostic perspectives in prostate cancer with the gastrin-releasing peptide receptor antagonist NeoBOMB1: Preclinical and first clinical results. *J Nucl Med*. 2017;58:75-80.

19. Maina T, Nock BA, Kulkarni H, Singh A, Baum RP. Theranostic Prospects of Peptide Receptor – Radioantagonists in Oncology. *Positron Emiss Tomogr*. 2017;12:297-309.

20. Mansi R, Wang X, Forrer F, et al. Development of a potent DOTA-conjugated bombesin antagonist for targeting GRPr-positive tumours. 2011:97-107.

21. Morgat C, MacGrogan G, Brouste V, et al. Expression of Gastrin-Releasing Peptide Receptor in Breast Cancer and Its Association with Pathologic, Biologic, and Clinical Parameters: A Study of 1,432 Primary Tumors. *Jounral Nucl Med*. 2017;58:1401-1408.

22. Stoykow C, Erbes T, Maecke HR, et al. Gastrin-releasing Peptide Receptor Imaging in Breast Cancer Using the Receptor Antagonist 68 Ga-RM2 And PET. *Theranostics*. 2016;6:1641-1650.

23. Mansi R, Minamimoto R, Iagaru AH. Bombesin-Targeted PET of Prostate Cancer. *Jounral Nucl Med*. 2016;57:67-73.

24. Lin KS, Luu A, Baidoo KE, et al. A new high affinity technetium-99m-bombesin analogue with low abdominal accumulation. *Bioconjug Chem*. 2005;16:43-50.

25. Nock BA, Nikolopoulou A, Galanis A, et al. Potent bombesin-like peptides for GRP-receptor targeting of tumors with 99mTc: A preclinical study. *J Med Chem.* 2005;48:100-110.

26. Figueroa SD, Volkert WA, Hoffman TJ. Evaluation of the Pharmacokinetic Effects of Various Linking Group Using the 111In-DOTA-X-BBN(7-14)NH2 Structural Paradigm in a Prostate Cancer Model. 2009;19:1803-1812.

27. García Garayoa E, Schweinsberg C, Maes V, et al. Influence of the molecular charge on the biodistribution of bombesin analogues labeled with the [99mTc(CO)3]-core. *Bioconjug Chem.* 2008;19:2409-2416.

28. Kurth J, Krause BJ, Schwarzenböck SM, Bergner C, Hakenberg OW, Heuschkel M. First-in-human dosimetry of gastrin-releasing peptide receptor antagonist [177Lu]Lu-RM2: a radiopharmaceutical for the treatment of metastatic castration-resistant prostate cancer. *Eur J Nucl Med Mol Imaging.* 2020;47:123-135.
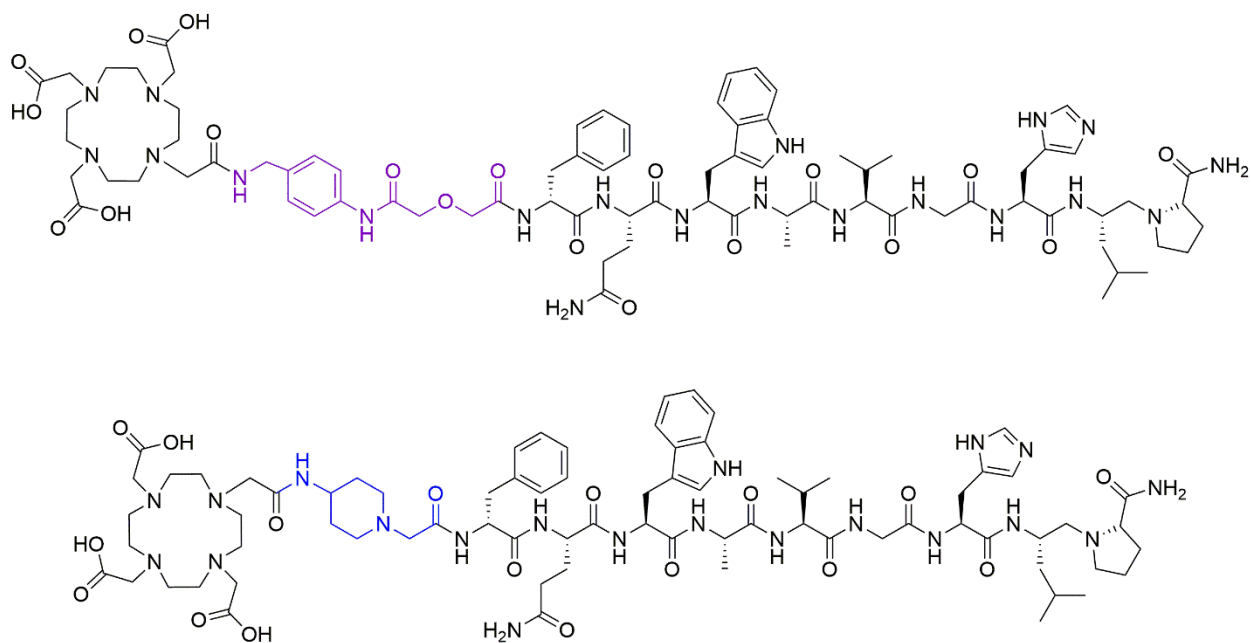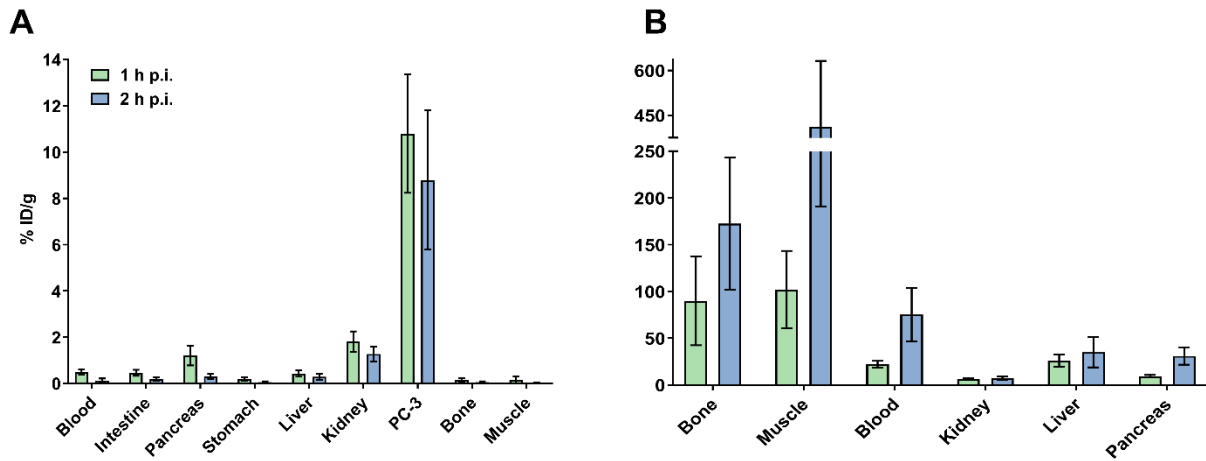
**Figure 1.** Chemical structure of ProBOMB1 (top) and ProBOMB2 (bottom)
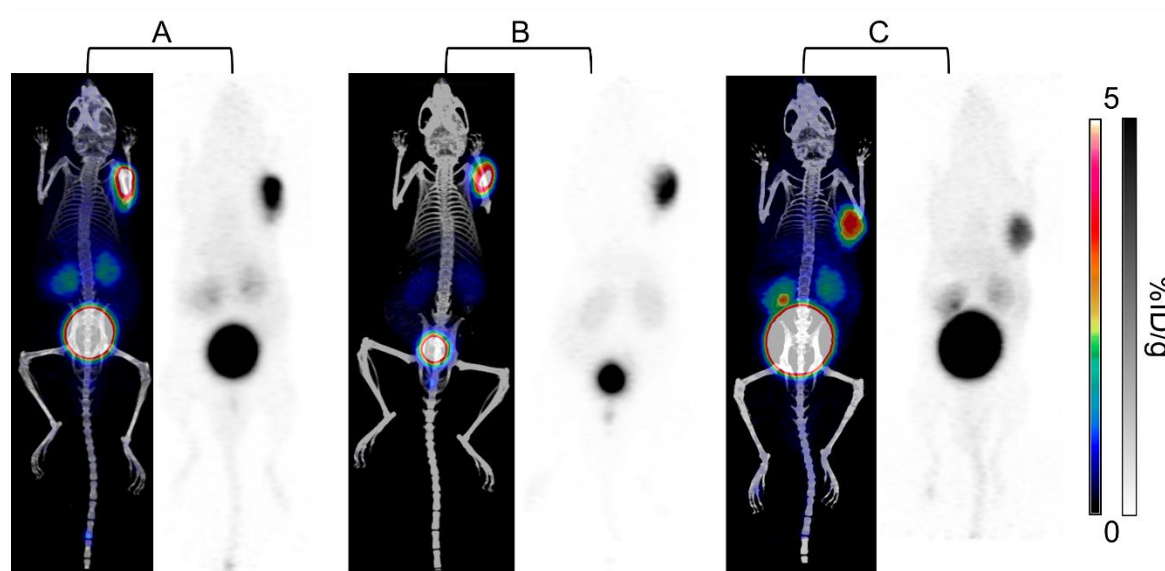
Figure 2. Fused MIP PET/CT and PET alone of ^{68}Ga-ProBOMB2 in PC-3 xenograft bearing mice. Acquired at (A) 1 h, (B) 2 h, and (C) 1 h with blocking p.i. Blocking was performed with co-injection of 100 μg of [D-Phe^6,Leu-NHEt^{13},des-Met^{14}]Bombesin(6-14).

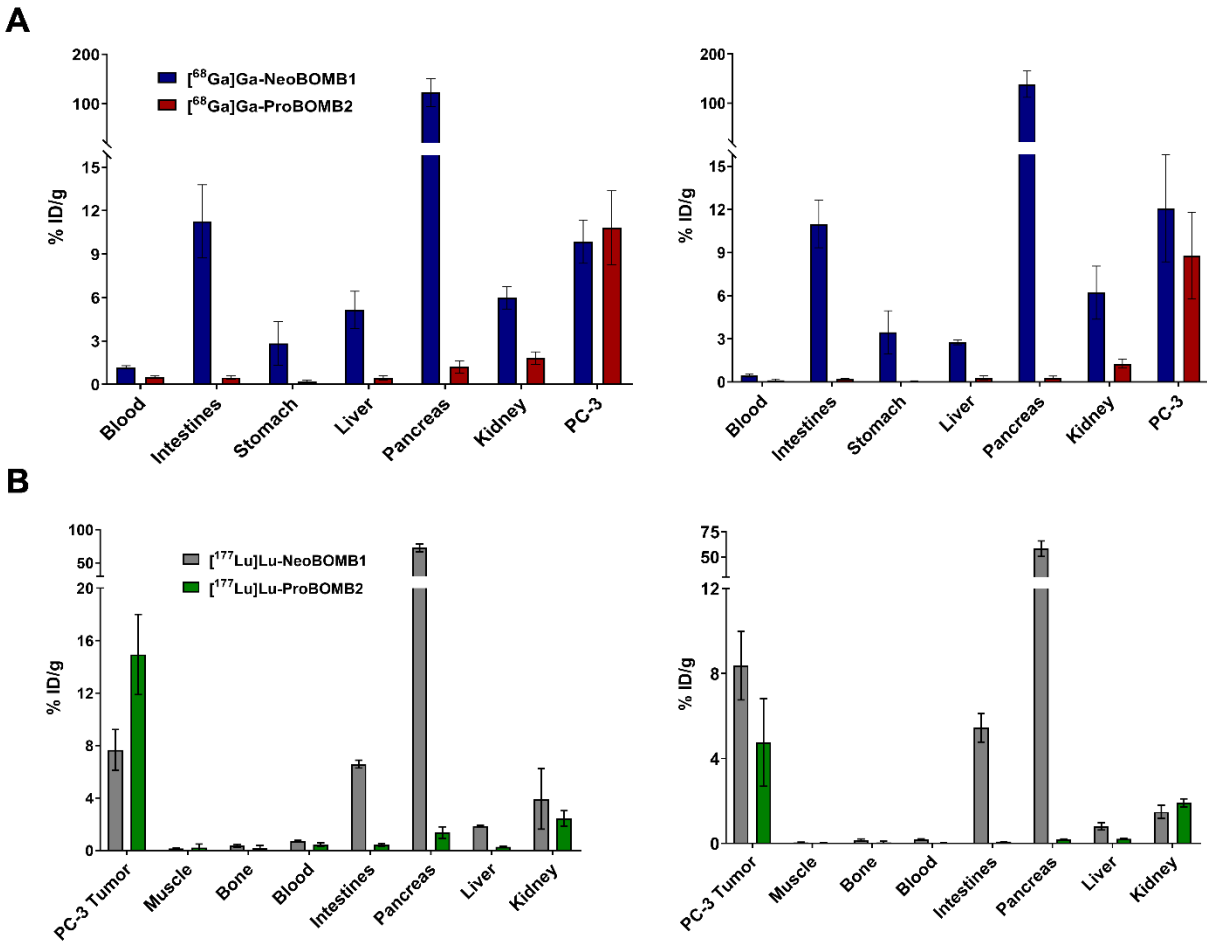**Figure 3.** Organ uptake (A) and tumor-to-organ ratios (B) of ^{68}Ga-ProBOMB2. Time points are at 1 h and

2 h p.i. in PC-3 xenograft bearing mice.
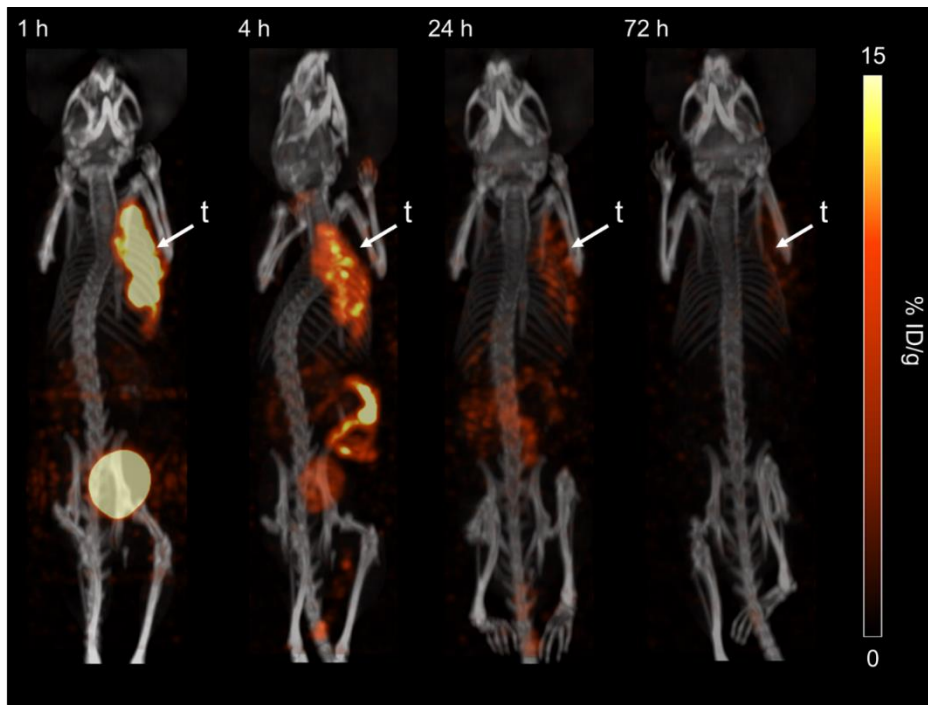
Figure 4. Fused MIP SPECT/CT of ^{177}Lu-ProBOMB2 in PC-3 xenograft bearing mice. Acquisition time

points are 1 h, 4 h, 24 h, and 72 h p.i. (t = tumor)
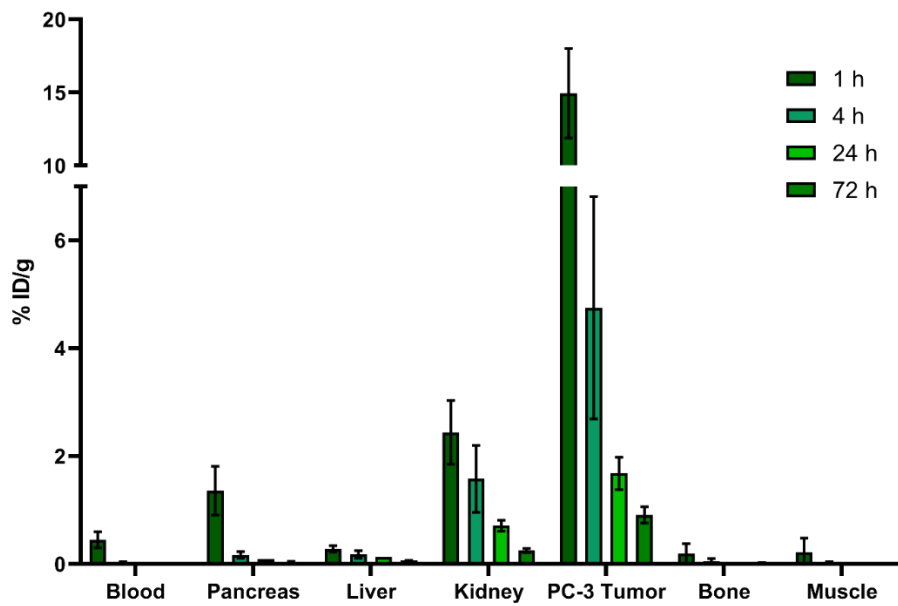
Figure 5. ^{177}Lu-ProBOMB2 uptake in organs of interest in PC-3 bearing mice

Figure 6. (A) Comparison of ^{68}Ga-ProBOMB2 and ^{68}Ga-NeoBOMB1 biodistributions in key organs in PC-3 tumor bearing mice. Biodistribution data is for 1 h p.i. (left) and 2 h p.i. (right)(*8*). (B) Comparison of ^{177}Lu-ProBOMB2 and ^{177}Lu-NeoBOMB1 uptake in key organs in PC-3 tumor bearing mice. Biodistribution data is for 1 h p.i. (left) and 4 h p.i. (right)(*7*).
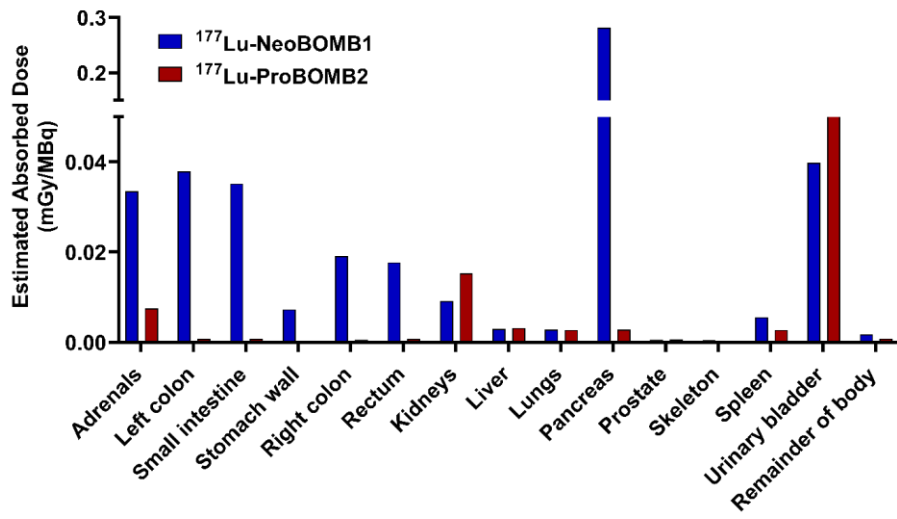
Figure 7. Estimated human absorbed doses of ^{177}Lu labeled NeoBOMB1 and ProBOMB2 for average adult male(*7*).

Table 1. Absorbed doses per unit of injected activity in mice for ^{177}Lu-ProBOMB2.

Target Organ	Absorbed Dose (mGy/MBq)
Brain	0.99
Large Intestine	2.17
Small Intestine	2.09
Stomach	1.89
Heart	2.24
Kidneys	42.70
Liver	9.34
Lungs	7.50
Pancreas	8.64
Bone	6.28
Spleen	8.15
Testes	2.76
Thyroid	0.83
Bladder	632.00
Remainder Body	5.64
Tumor	134.63

Table 2. Estimated organ absorbed doses of ^{177}Lu-ProBOMB2 for an adult human male.

Target Organ	Absorbed Dose (mGy/MBq)
Adrenals	7.51E-03
Brain	7.43E-05
Esophagus	3.18E-04
Eyes	2.57E-04
Gallbladder Wall	3.91E-04
Left colon	7.57E-04
Small Intestine	7.54E-04
Stomach Wall	3.67E-04
Right colon	5.48E-04
Rectum	7.06E-04
Heart	7.45E-04
Kidneys	1.53E-02
Liver	3.15E-03
Lungs	2.75E-03
Pancreas	2.82E-03
Prostate	6.09E-04
Salivary Glands	2.65E-04
Red Marrow	3.45E-04
Skeleton	4.72E-04
Spleen	2.73E-03
Testes	6.96E-04
Thymus	2.96E-04
Thyroid	2.84E-04
Urinary Bladder	5.27E-02
Remainder Body	8.03E-04

Graphical Abstract
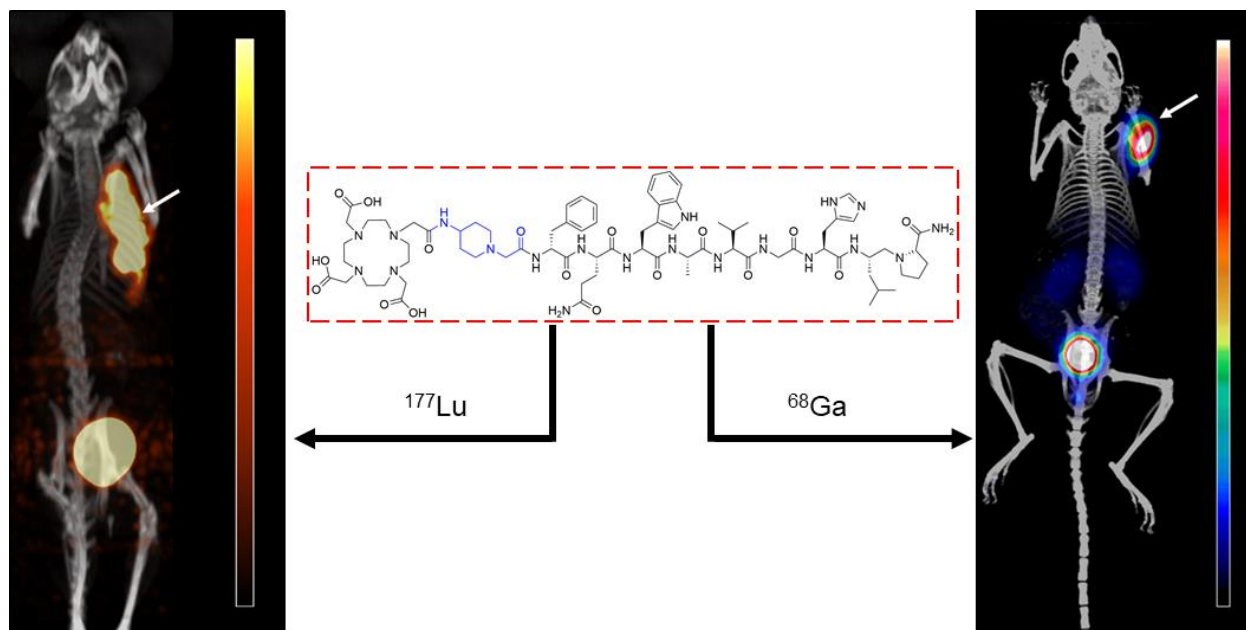
SUPPLEMENTARY INFORMATION

SYNTHESIS AND ANALYSIS OF PROBOMB2 AND DERIVATIVES

Chemicals and Instrumentation

All reagents and solvents were purchased from commercial sources and used without further purification. [D-Phe[6],Leu-NHEt[13],des-Met[14]]Bombesin(6-14) and bombesin were purchased from Bachem and Anaspec, respectively. Other peptides were synthesized on an AAPPTec Endeavor 90 peptide synthesizer. Purification and quality control of synthesized materials were performed using high-performance liquid chromatography (HPLC) with a semi-preparative column (Phenomenex, Luna®, C18, 5 μm, 250 × 10 mm) or an analytical column (Phenomenex, Luna®, C18, 5 μm, 250 × 4.6 mm), respectively, on an Agilent 1260 infinity system. Small molecule purification was carried out using HPLC with a preparative column (Phenomenex, Gemini®, NX-C18, 5 μm, 50 × 30 mm), using an Agilent 1260 Infinity II system. HPLC systems were equipped with Infinity Diode Array Detector (DAD, UV to VIS) and/or a Bioscan NaI scintillation detector. Mass analyses were conducted using a TripleTOF 5600 mass spectrometer (AB/Sciex). [68]Ga was eluted from an iThemba Labs generator and purified according to previously published procedures using a DGA resin column from Eichrom Technologies LLC[11]. Radioactivity of ^{68}Ga-labeled peptides was measured using a Capintec CRC-25R/W dose calibrator, and the radioactivity in tissues collected from biodistribution studies was counted using a Perkin Elmer Wizard2 2480 gamma counter. [177]LuCl$_3$ was purchased from ITG.

Synthesis of Fmoc-LeuψPro-OH

Fmoc-Leucinol (1.1 g, 3.24 mmol) in 50 ml dichloromethane was stirred with Dess-Martin Periodinane (2.7 g, 6.36 mmol) at room temperature for 4 hours. The reaction mixture was concentrated *in vacuo* before adding hexanes (70 mL) and saturated sodium bicarbonate solution (30 mL) and stirring for 15 minutes before filtering. The filtrate was washed with saturated sodium bicarbonate solution (3x 50 mL), water (3x 50 mL), and brine (3x 50 mL). The organic layer was collected and dried over magnesium sulfate, filtered, and evaporated *in vacuo* to obtain crude crystalline compound. The isolated solid was dissolved in 36 mL dichloroethane with L-Proline (410 mg, 3.56 mmol) and the mixture stirred for 48 h at room temperature. Sodium triacetoxyborohydride (1.7 g, 8.1 mmol) was added to the mixture and stirred further

for 16 h. The solution was then concentrated *in vacuo* and ethyl acetate and saturated sodium bicarbonate was added (1:1, 50 mL) and the mixture stirred for 10 min. The organic layer was washed with saturated sodium bicarbonate solution (3x 50 mL), water (3x 50 mL), and brine (3x 50 mL). The organic layer was dried over MgSO$_4$ before concentrated under vacuum to obtain yellow crude solid. Crude material was purified using HPLC (Phenomenex Gemini Prep column, 38% acetonitrile and 0.1% TFA in water, flow rate 30 mL/min). Retention time: 9.8 min. Product peak was collected and lyophilized to obtain the product as white powder (yield: 436 mg, 31% yield). ESI-MS: calculated [M+H]$^+$ for Fmoc-LeuψPro-OH C$_{26}$H$_{32}$N$_2$O$_4$ 437.2; found 437.3.

Synthesis of ProBOMB2

ProBOMB2 was synthesized on solid-phase using Fmoc-based approach. Rink amide-MBHA resin (0.1 mmol) was treated with 20% piperidine in *N,N*-dimethylformamide (DMF) to remove Fmoc protecting group. Fmoc-LeuψPro-OH pre-activated with HATU (3 eq), HOAt (3 eq), and *N,N*-diisopropylethylamine (DIEA, 6 eq) was coupled to the resin. After removal of Fmoc protecting group, Fmoc-His(Trt)-OH, Fmoc-Gly-OH, Fmoc-Val-OH, Fmoc-Ala-OH, Fmoc-Trp(Boc)-OH, Fmoc-Gln(Trt)-OH, Fmoc-D-Phe-OH, Fmoc-4-amino-(1-carboxymethyl) piperidine and DOTA (pre-activated with HATU (3 eq), HOAt (3 eq) and DIEA (6 eq)) were coupled to the resin sequentially. The peptide was deprotected and cleaved from the resin with a mixture of trifluoroacetic acid (TFA) 92.5%, triisopropylsilane (TIS) 2.5%, water 2.5%, 2,2′-(ethylenedioxy)diethanethiol (DODT) 2.5% for 3 h at room temperature. After filtration, the peptide was precipitated by addition of cold diethyl ether, collected by centrifugation, and purified by HPLC (semi-preparative column; 20% acetonitrile and 0.1% TFA in water, flow rate: 4.5 mL/min). The isolated yield was 2.4%. Retention time: 16.8 min. ESI-MS: calculated [M+2H]$^+$ for C$_{75}$H$_{112}$N$_{20}$O$_{17}$Ga ProBOMB2: 1567.8; found 1567.4.

Synthesis of Non-Radioactive Ga- and Lu- Coupled ProBOMB2

ProBOMB2 (1.8 mg, 1.15 µmol) and GaCl$_3$ (0.2 M, 28.5 µL, 5.75 µmol) in 450 µL sodium acetate buffer (0.1 M, pH 4.2) were incubated at 80°C for 30 min, and purified by HPLC using the semi-preparative column (20% acetonitrile and 0.1% TFA in water; flow rate: 4.5 mL/min). The isolated yield was 88%. Retention time: 12.1 min. ESI-MS: calculated [M+H]$^+$ for Ga-ProBOMB2 C$_{75}$H$_{110}$N$_{20}$O$_{19}$Ga 1631.7; found 1631.9. ProBOMB2 (1.36 mg, 0.869 µmol) and LuCl$_3$ (0.2 M, 21.7 µL, 4.3455 µmol) in 450

μL sodium acetate buffer (0.1 M, pH 4.2) was incubated at 80°C for 30 min, and purified by HPLC using the semi-preparative column (21% acetonitrile and 0.1% TFA in water; flow rate: 4.5 mL/min. The isolated yield was 86%. Retention time: 8.6 min. ESI-MS: calculated $[M+H]^+$ for Lu-ProBOMB2 $C_{75}H_{110}N_{20}O_{17}Lu$ 1738.7; found 1738.7.

Radiolabeling of ProBOMB2

^{68}Ga-ProBOMB2: Purified ^{68}GaCl$_3$ (289 – 589 MBq, in 0.5 mL water) was added to 0.5 mL of HEPES buffer (2 M, pH 5.4) containing ProBOMB2 (25 μg) and this solution was heated by microwave. Unlabeled ProBOMB2 and ^{68}Ga-ProBOMB2 were separated by HPLC to ensure high molar activity of the labeled product for mouse studies (Phenomenex, Luna®, C18, 5 μm, 250 × 10 mm); isocratic 21% acetonitrile and 0.1% TFA in water; flow rate: 4.5 mL/min). The ^{68}Ga-ProBOMB2 containing fraction was collected, diluted with water, and trapped on a C18 Sep-Pak cartridge. The trapped ^{68}Ga-ProBOMB2 was air dried, eluted with ethanol, and diluted with phosphate-buffered saline (PBS). A C18 analytical column was used to perform quality control (Phenomenex, Luna®, C18, 5 μm, 250 × 4.6 mm; 25% acetonitrile (0.1% TFA) and 75% H_2O (0.1% TFA), 2.0 mL/min, retention time 6.3 min).

^{177}Lu-ProBOMB2: ^{177}Lu, obtained as ^{177}LuCl$_3$ in solution from ITG, was added to 25 μg of ProBOMB2 in 0.5 mL of sodium acetate buffer (0.1M; pH 4.5) and incubated at 95°C for 15 minutes in a water bath. ^{177}Lu-ProBOMB2 was isolated from uncomplexed ^{177}Lu and ProBOMB2 using HPLC, semipreparative column (same as above), with 20% acetonitrile (0.1% TFA) in water with a flow rate of 4.5 mL/min. The retention time of the product was 25 min. Quality control was done using the same analytical column mentioned above (22% acetonitrile (0.1% TFA) and 78% H_2O (0.1% TFA), 2.0 mL/min, retention time 10.3 min).

Fluorometric Calcium Release Assay

Based on published procedures, 5 x 10^4 PC-3 cells were seeded in 96-well clear bottom black plates. The growth medium was removed and a loading buffer containing a calcium-sensitive dye was added. After incubating for 30 mins at 37°C, the plates were placed in a FlexStation 3 microplate reader (Molecular Devices). Ga-ProBOMB2 (50 nM), Lu-ProBOMB2 (50 nM), [D-Phe^6,Leu-NHEt^{13},des-Met^{14}]Bombesin(6-14) (50 nM), bombesin (50 nM), ATP (positive control) (50 nM), or PBS (negative

control) were added to the cells and the fluorescent signals acquired for 120 s. Agonistic/antagonistic properties were determined using the relative fluorescent unit (RFU = max – min).
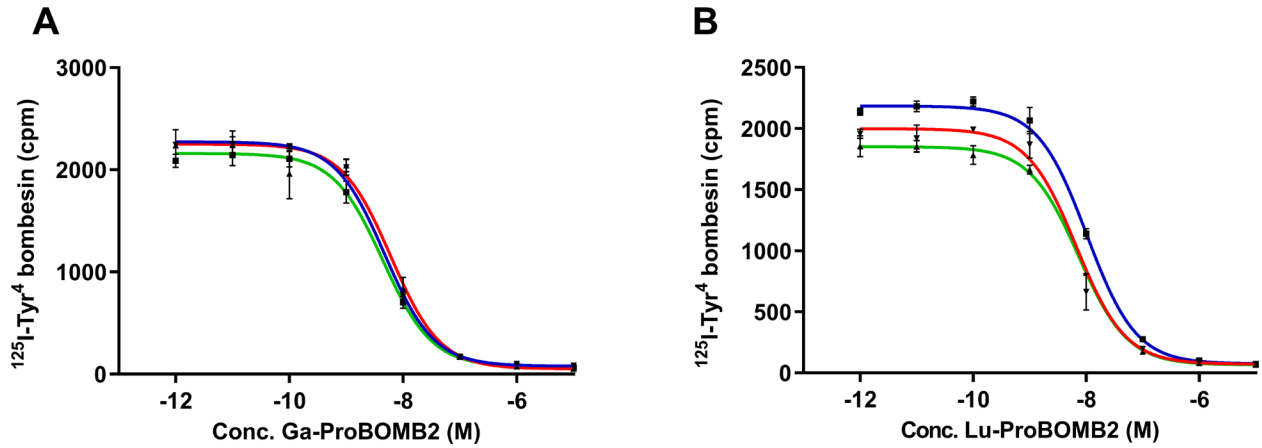
Supplemental Figure 1. Displacement curves of ^{125}I-Tyr^{4}Bombesin by Ga-ProBOMB2 (A) and Lu-ProBOMB2 (B) on human GRPR expressing PC-3 cells.
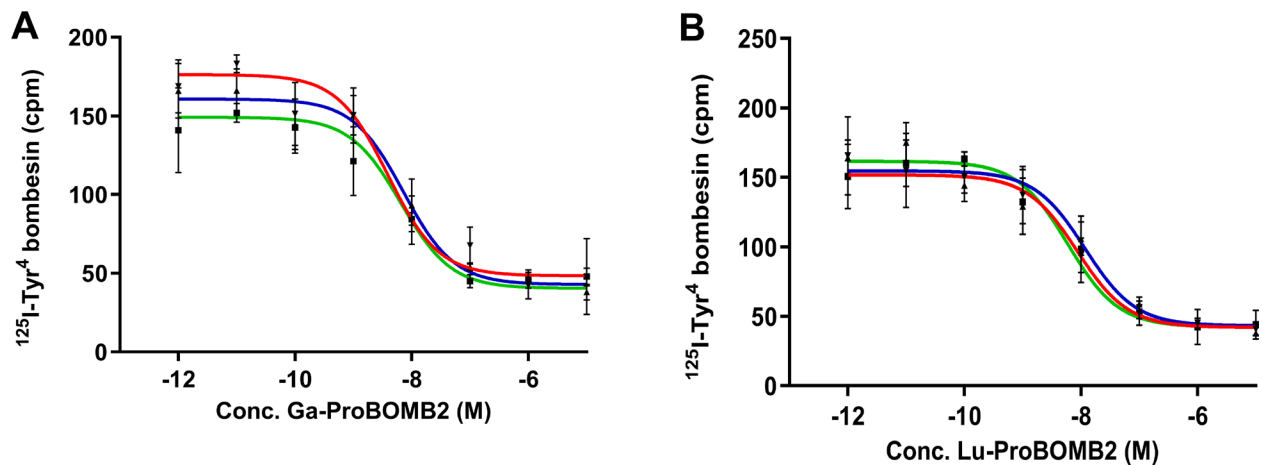
Supplemental Figure 2. Displacement curves of ^{125}I-Tyr^{4}Bombesin by Ga-ProBOMB2 (A) and Lu-ProBOMB2 (B) on murine GRPR expressing Swiss 3T3 cells.
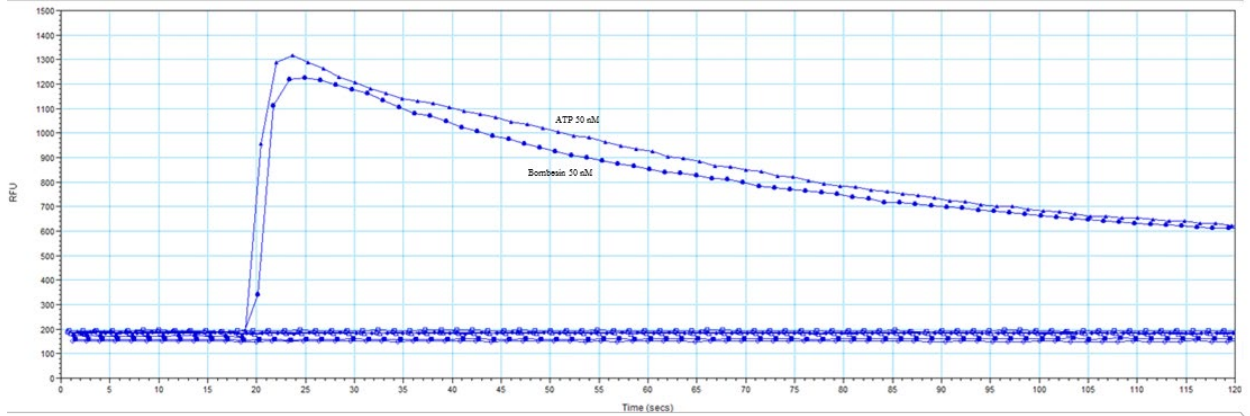
Supplemental Figure 3. Representative FLIPR Calcium 6 release assay in PC-3 cells. Cells were incubated with Ga-ProBOMB2, Lu-ProBOMB2, ([D-Phe^6,Leu-NHEt^{13},des-Met^{14}]Bombesin(6-14)], Bombesin, ATP, or PBS control. The y-axis is relative fluorescence unit (RFU) and the x-axis is time (sec).
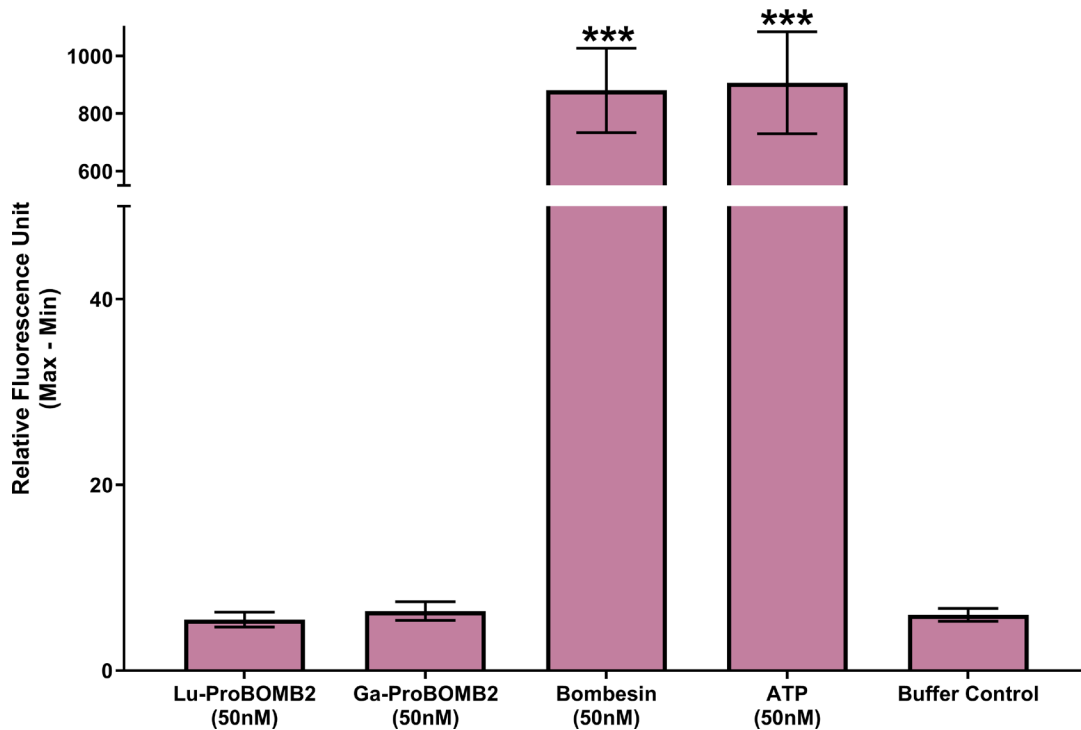
Supplemental Figure 4. Intracellular calcium efflux in PC-3 cells. Cells were incubated with 50 nM of Ga-ProBOMB2, Lu-ProBOMB2, [D-Phe^6,Leu-NHEt^{13},des-Met^{14}]bombesin(6-14), bombesin, ATP, or buffer control. ***$p \leq 0.05$ compared with buffer control.

Supplemental Table 1. Biodistribution and tumor-to-organ contrasts of ^{68}Ga-ProBOMB2 in PC-3 xenograft bearing mice at 60 min and 120 min post-injection

Tissues	1 h (%ID/g) (n = 6)		2 h (%ID/g) (n = 7)		1 h Blocked* (%ID/g) (n = 6)	
	Mean	SD	Mean	SD	Mean	SD
PC-3 Tumor	10.80	2.56	8.79	3.01	3.77	0.92
Urine	586.50	235.13	152.14	129.63	612.80	379.28
Blood	0.49	0.11	0.13	0.08	0.53	0.15
Fat	0.06	0.02	0.02	0.01	0.08	0.03
Seminal	2.44	2.53	1.63	2.88	1.95	2.37
Testes	0.16	0.06	0.07	0.05	0.21	0.08
Intestine	0.46	0.13	0.19	0.08	0.34	0.12
Spleen	0.27	0.12	0.11	0.03	0.33	0.17
Pancreas	1.20	0.42	0.30	0.11	0.62	0.19
Stomach	0.19	0.08	0.06	0.03	0.07	0.02
Liver	0.43	0.14	0.29	0.13	0.57	0.18
Adrenal Glands	0.76	0.58	0.47	0.31	0.32	0.17
Kidney	1.81	0.44	1.27	0.31	2.22	0.79
Heart	0.18	0.04	0.05	0.02	0.16	0.03
Lungs	0.39	0.10	0.13	0.04	0.41	0.09
Bone	0.15	0.08	0.06	0.03	0.13	0.09
Muscle	0.15	0.15	0.03	0.02	0.09	0.04
Brain	0.02	0.00	0.01	0.00	0.02	0.00
Tail	0.38	0.10	0.14	0.08	0.68	0.27
Tumor to Normal Tissue Ratios						
	1 h		2 h		1 h Blocked*	
Blood	22.19	3.51	75.32	28.59	7.23	1.40
Muscle	101.99	41.47	411.17	220.57	43.96	8.26
Kidney	6.03	0.88	6.96	1.89	1.77	0.39
Pancreas	9.32	1.38	31.05	9.28	6.17	1.09
Liver	26.18	6.43	34.99	16.10	7.33	2.89
Bone	89.90	47.46	172.53	70.48	39.81	21.70

*Mice received a co-injection of 100 µg of [D-Phe[6],Leu-NHEt[13],des-Met[14]]Bombesin(6-14).

Supplemental Table 2. Biodistribution and tumor-to-organ contrasts of ^{177}Lu-ProBOMB2 in PC-3 xenograft bearing mice at 1 h, 4 h, and 24 h post-injection

Tissues	1 h (%ID/g) (n = 9) Mean	SD	4 h (%ID/g) (n = 8) Mean	SD	24 h (%ID/g) (n = 7) Mean	SD	72 h (%ID/g) (n = 7) Mean	SD	1 h Blocked* (%ID/g) (n = 4) Mean	SD
PC-3 Tumor	14.94	3.06	4.75	2.06	1.68	0.30	0.91	0.15	3.10	1.13
Urine	583.93	368.57	46.32	51.39	0.68	0.30	0.20	0.05	331.66	204.20
Blood	0.45	0.15	0.03	0.01	0.01	0.00	0.00	0.00	0.40	0.11
Fat	0.12	0.15	0.01	0.01	0.01	0.00	0.01	0.00	0.07	0.01
Seminal	0.15	0.23	0.12	0.32	0.01	0.00	0.00	0.00	4.80	9.49
Testes	0.26	0.24	0.02	0.01	0.02	0.00	0.01	0.00	0.12	0.02
Intestine	0.43	0.10	0.09	0.05	0.20	0.40	0.09	0.09	0.26	0.07
Spleen	0.33	0.17	0.08	0.03	0.08	0.00	0.06	0.02	0.23	0.06
Pancreas	1.36	0.45	0.17	0.06	0.09	0.00	0.04	0.01	0.46	0.23
Stomach	0.15	0.06	0.02	0.01	0.31	0.70	0.21	0.31	0.12	0.08
Liver	0.28	0.06	0.18	0.07	0.13	0.00	0.06	0.01	0.28	0.05
Adrenal Glands	0.88	0.73	0.46	0.40	0.26	0.10	0.16	0.11	0.18	0.10
Kidney	2.44	0.59	1.58	0.62	0.71	0.10	0.25	0.04	2.92	0.61
Heart	0.15	0.05	0.03	0.01	0.02	0.00	0.01	0.00	0.14	0.03
Lungs	1.24	0.80	0.31	0.31	0.11	0.10	0.04	0.03	0.43	0.05
Bone	0.19	0.19	0.05	0.05	0.03	0.00	0.02	0.01	0.18	0.13
Muscle	0.22	0.26	0.02	0.02	0.01	0.00	0.00	0.00	0.12	0.10
Brain	0.03	0.03	0.01	0.00	0.00	0.00	0.00	0.00	0.02	0.00
Tail	1.18	0.90	0.35	0.20	0.42	0.30	0.14	0.11	0.82	0.36

Tumor to Normal Tissue Ratios

	1 h		4 h		24 h		72 h		1 h Blocked*	
Blood	35.34	8.47	184.30	55.92	320.13	160.30	687.87	178.06	7.63	1.11
Muscle	121.92	77.29	456.57	287.93	222.28	56.60	229.59	99.05	31.81	10.19
Kidney	6.33	1.60	3.22	0.93	2.39	0.30	3.62	0.48	1.04	0.15
Pancreas	11.70	3.08	29.85	7.95	19.57	4.00	25.83	5.83	7.09	0.82
Liver	54.73	12.31	28.72	8.22	13.77	4.50	14.97	3.10	11.05	2.33
Bone	148.51	92.51	150.00	80.94	71.80	34.00	63.73	42.35	22.96	12.81

*Mice received a co-injection of 100 µg of [D-Phe[6],Leu-NHEt[13],des-Met[14]]Bombesin(6-14).